

Classification of Bounded Travelling Wave Solutions of the General Burgers-Boussinesq Equation

*Rasool Kazemi * and Masoud Mosaddeghi*

Abstract

By using bifurcation theory of planar dynamical systems, we classify all bounded travelling wave solutions of the general Burgers-Boussinesq equation, and we give their corresponding phase portraits. In different parametric regions, different types of travelling wave solutions such as solitary wave solutions, cusp solitary wave solutions, kink (anti kink) wave solutions and periodic wave solutions are simulated. Also in each parameter bifurcation sets, we obtain the exact explicit parametric representation of all travelling wave solutions.

Keywords: General Burgers-Boussinesq equation, travelling wave solutions, Bifurcation theory.

2010 Mathematics Subject Classification: 34C25, 35B32.

How to cite this article

R. Kazemi and M. Mosaddeghi, Classification of bounded travelling wave solutions of the general Burgers-Boussinesq equation, *Math. Interdisc. Res.* 4 (2019) 263 – 279.

1. Introduction

Nonlinear partial differential equations (NPDEs) have a wide array of applications in many fields. For example it can describe the motion of the isolated waves localized in a small part of space. Also it can be applied in physics and engineering for expressing the behavior of magneto fluid dynamics, water surface gravity waves, electromagnetic radiation reactions, and ion acoustic waves. Finding explicit exact solution of NPDEs plays an important role in the study of nonlinear

*Corresponding author (E-mail: r.kazemi@kashanu.ac.ir)
Academic Editor: Abbas Saadatmandi
Received 23 April 2016, Accepted 12 June 2016
DOI: 10.22052/mir.2016.33673

physical phenomena. In recent years, numerous powerful and direct methods for finding the explicit solutions of NPDE have been developed, such as Hirota bilinear method [7], Backlund transformation method [14], Painleve expansion method [17], Sine-Cosine method [18], homotopy perturbation method [6], homogenous balance method [16], algebraic method [8], Jacobi elliptic function expansion method [12], F-expansion method [2, 3, 13], and so on. It should be mentioned that bifurcation theory of planar dynamical systems is an efficient method as well [4, 9, 11, 19, 20]. In this paper, we consider the following general Burgers-Boussinesq equations

$$\begin{aligned}u_t &= (\alpha/2)v_{xxx} - (\beta/2)u_{xx} + 2(uv)_x, \\v_t &= (\beta/2)v_{xx} + 2vv_x + (1/2)u_x,\end{aligned}\tag{1}$$

where α and β are real parameters and system (1) describe water waves. Finding it's travelling wave solutions is very helpful for mechanical and civil engineers to apply the nonlinear water model in harbor and coastal design. In [10] by using the extended homogenous balance method the exact travelling waves and the soliton wave solutions of Burges-Boussinesq equations were obtained. Also in [15] by the Jacobi elliptic function method, the periodic wave solutions for Burges-Boussinesq equations were obtained. We will find exact solutions of (1) using the bifurcation theory of planar dynamical systems. The purpose of this paper is to give the bifurcation sets of the bounded travelling wave solutions, i.e. solitary wave solutions, kink (anti kink) wave solutions and periodic wave solutions. Also we obtain the explicit representation for some of these solutions in different parametric region determined by the bifurcation set. To find the travelling wave solutions of (1) we consider the travelling wave solution of the form:

$$u(x, t) = u(\xi), \quad v(x, t) = v(\xi), \quad \xi = x - ct,\tag{2}$$

where c is an arbitrary constant and denotes the wave speed. By substituting for u and v from (2) into the equations (1) we get the following ordinary differential equations:

$$\begin{aligned}-cu_\xi - (\alpha/2)v_{\xi\xi\xi} + (\beta/2)u_{\xi\xi} - 2(uv)_\xi &= 0, \\-cv_\xi - (\beta/2)v_{\xi\xi} - 2vv_\xi - (1/2)u_\xi &= 0.\end{aligned}\tag{3}$$

By integration of (3) once with respect to ξ we obtain

$$\begin{aligned}-cu - (\alpha/2)v_{\xi\xi} + (\beta/2)u_\xi - 2(uv) &= -g_1, \\-cv - (\beta/2)v_\xi - v^2 - (1/2)u &= -g_2,\end{aligned}\tag{4}$$

where g_1 and g_2 are real integral constants. From the second equation of (4), we get

$$\begin{aligned}u &= 2g_2 - 2cv - \beta v_\xi - 2v^2, \\u_\xi &= -2cv_\xi - \beta v_{\xi\xi} - 4vv_\xi.\end{aligned}\tag{5}$$

Now we substitute u and u_ξ from (5) into the first equation of (4) to obtain

$$(\alpha + \beta^2) v_{\xi\xi}/2 - 4v^3 - 6cv^2 + 2(2g_2 - c^2)v + (2cg_2 - g_1) = 0. \quad (6)$$

If $\alpha + \beta^2 = 0$, system (6) is reduced to algebraic equation

$$-4v^3 - 6cv^2 + 2(2g_2 - c^2)v + (2cg_2 - g_1) = 0. \quad (7)$$

In this case we have constant travelling waves which correspond to zeros of (7) where the number of its zeros will change from one to three by changing the parameters. To consider the nontrivial case we assume that $\alpha + \beta^2 \neq 0$. Now let $dv/d\xi = x_2$. Then we derive the following travelling wave system which is a planar Hamiltonian system:

$$\begin{aligned} \frac{dv}{d\xi} &= x_2, \\ \frac{dx_2}{d\xi} &= \frac{2}{\alpha + \beta^2} (4v^3 + 6cv^2 - 2(2g_2 - c^2)v - 2cg_2 + g_1). \end{aligned} \quad (8)$$

The phase portraits of the Hamiltonian system (8) determine all travelling wave solutions of (1), so we want to find the bifurcation set for which the qualitative behavior of phase portraits of (8) changes. Here we consider only bounded travelling waves, because in physical models only bounded travelling waves are meaningful.

Suppose that $v(x, t) = v(x - ct) = v(\xi)$ is a continuous solution of system (8) for $-\infty < \xi < \infty$ and $\lim_{\xi \rightarrow +\infty} v(\xi) = p$, $\lim_{\xi \rightarrow -\infty} v(\xi) = q$. We recall that

- (i) if $p = q$ then $v(x, t)$ is called a solitary or impulse wave solution, and
- (ii) if $p \neq q$ then $v(x, t)$ is called kink (anti kink) wave solution.

Usually a solitary wave solution, a kink (anti kink) wave and periodically travelling wave solution of equations (1) corresponds to a homoclinic orbits or cuspidal loop, heteroclinic orbit and periodic orbit of (8) respectively. Thus we need to find all periodic, homoclinic orbits, cuspidal loop and heteroclinic orbits of system (8) which depend on the system's parameters.

The rest of this paper is organized as follows. In section 2, we give the bifurcation set and corresponding phase portrait of system (8). In Section 3, using the information obtained about the phase portraits of bounded solution of (8) we obtain the numerical simulation for corresponding bounded travelling wave solutions of the system (1). In Section 4, we give exact explicit parametric representation for different possible solitary wave solution, periodic travelling wave solution and kink (anti kink) wave solution of equation (1).

2. Bifurcation Diagram of System (8)

In this section, we consider bifurcation set and phase portraits of (8). To simplify our analysis, we make the following change of coordinates which remove second

order term in (8). Let $x_1 = v + c/2$, then (8) becomes

$$\begin{aligned}\frac{dx_1}{d\xi} &= x_2, \\ \frac{dx_2}{d\xi} &= f(\lambda, \mu, x_1),\end{aligned}\tag{9}$$

where $f(\lambda, \mu, x_1) = \frac{8}{\alpha + \beta^2}(\lambda + \mu x_1 + x_1^3)$, $\lambda = g_1/4$ and $\mu = -g_2 - c^2/4$. System (9) is Hamiltonian system with Hamiltonian $H(\lambda, \mu, x_1, x_2) = x_2^2/2 + F(\lambda, \mu, x_1)$, where

$$F(\lambda, \mu, x_1) = \frac{-8}{\alpha + \beta^2}(\lambda x_1 + \mu x_1^2/2 + x_1^4/4),\tag{10}$$

is the potential function of the Hamiltonian system (9). Critical points of F are zeros of f . It is known that isolated minimum, maximum and inflection points of F correspond to center, saddle point and cusp point of system (9) respectively (e.g. see [5]). Also it is known that the global structure of phase portraits of system (9) will not change qualitatively unless one of the conditions listed below is violated [5]:

- i) There are only finitely many critical points of F .
- ii) Each critical point of F is non-degenerate, that is $F''(\bar{x}_1) \neq 0$ for all critical points \bar{x}_1 .
- iii) No two maximum values of F are equal.
- iv) $|F(x_1)| \rightarrow \infty$ as $|x_1| \rightarrow \infty$, that is F is unbounded for both $x_1 \rightarrow \infty$ and $x_1 \rightarrow -\infty$.

A potential function that satisfies the above four conditions is called a generic potential function. In our case it is clear that the conditions (i) and (iv) are satisfied for all values of λ and μ . Therefore to find the bifurcation set, we first need to find conditions where critical points of F becomes degenerate. So we set

$$\begin{aligned}f(\lambda, \mu, x_1) &= \lambda + \mu x_1 + x_1^3 = 0, \\ f_{x_1}(\lambda, \mu, x_1) &= \mu + 3x_1^2 = 0.\end{aligned}\tag{11}$$

From (11) and finding μ and λ in terms of x_1 and then cancelling x_1 among them one can find the bifurcation curve

$$\Gamma := \{(\lambda, \mu) : \lambda^2 = -(4/27)\mu^3\} = \{(g_1, g_2, c) : g_1^2 = (c^2 + 4g_2)^3/27\},$$

where Γ is a cusp in λ - μ parameter plane which divides the plane into five distinct regions (see Figures 1 and 2). In each parametric region, number and type of critical points remains unchanged. To see the type and number of critical points it

is sufficient to consider a typical equation for a particular value of μ and λ in that region. It is easy to verify that number of critical points of F will change from one non-degenerate critical point to three non-degenerate critical points as parameters move from region (I) (outside of the cusp) into region (III) (inside the cusp). For parameter values on the cusp, the potential function has two critical points, one of them is a non-degenerate critical point and the other is degenerate, also for $\mu = \lambda = 0$ where two branch of the cusp intersect, there is only one degenerate critical point. To classify non-degenerate critical points and determine the phase portraits of system (9) we need to consider two cases ($\alpha + \beta^2 > 0$) and ($\alpha + \beta^2 < 0$) separately.

Case I: $\alpha + \beta^2 > 0$.

Since F is a polynomial of order four and the coefficient of x_1^4 is negative, it is easy to verify that the only non-degenerate critical points of F in region I (outside of the cusp) is a maximum point. Inside the cusp (region III) the potential function always has two non-degenerate maximum points and a non-degenerate minimum point between them, but the flow of system (9) is not equivalent for all parameter values. Indeed there are parameter values at which the two maxima of potential functions have the same maximum values for which the condition (ii) above for generic potential function is violated. The value of potential function at these two maximum points are equal only if $\lambda = 0$, $\mu < 0$ ($g_1 = 0, c^2 + 4g_2 > 0$) where the system (9) has a heteroclinic cycle. For $\lambda \neq 0$ inside the cusp (region III(a, c)) the system (9) has a homoclinic orbit surrounding the center. As parameter values cross the negative μ axis (region III(b)), the homoclinic orbit turn into two heteroclinic orbits and then back to a homoclinic orbit again. In region V where $\lambda = \mu = 0$ we have a degenerate maximum point. Typical graph of potential function and the corresponding phase portraits of system (9) are given in Figure 1 for different parametric regions. Therefore we have proved:

Theorem 2.1. Consider system (9) and assume that $\alpha + \beta^2 > 0$, then we have

- (1) If $\lambda^2 > -4\mu^3/27$, ($g_1^2 > (c^2 + 4g_2)^3/27$) (region I), the potential function (10) has only one maximum point and corresponding system (9) has a saddle point and all trajectories are unbounded (see Figure 1(I)).
- (2) If $\lambda^2 = -4\mu^3/27$, $\lambda \neq 0$, ($g_1^2 = (c^2 + 4g_2)^3/27$, $g_1 \neq 0$) (regions II and IV), the potential function (10) has an inflection point and a maximum point and the corresponding system (9) has a saddle and a cusp point. Again all trajectories are unbounded (see Figure 1 (II, IV)).
- (3) If $\lambda^2 < -4\mu^3/27$, $\lambda \neq 0$, ($g_1^2 < (c^2 + 4g_2)^3/27$, $g_1 \neq 0$) (regions III(a) and III(b)), the potential functions (10) has a minimum and two maximum points, which correspond to a center and two saddle points of (9) respectively and the values of potential function (10) at maximum points are not equal. The corresponding system (9) has a homoclinic orbit which is filled

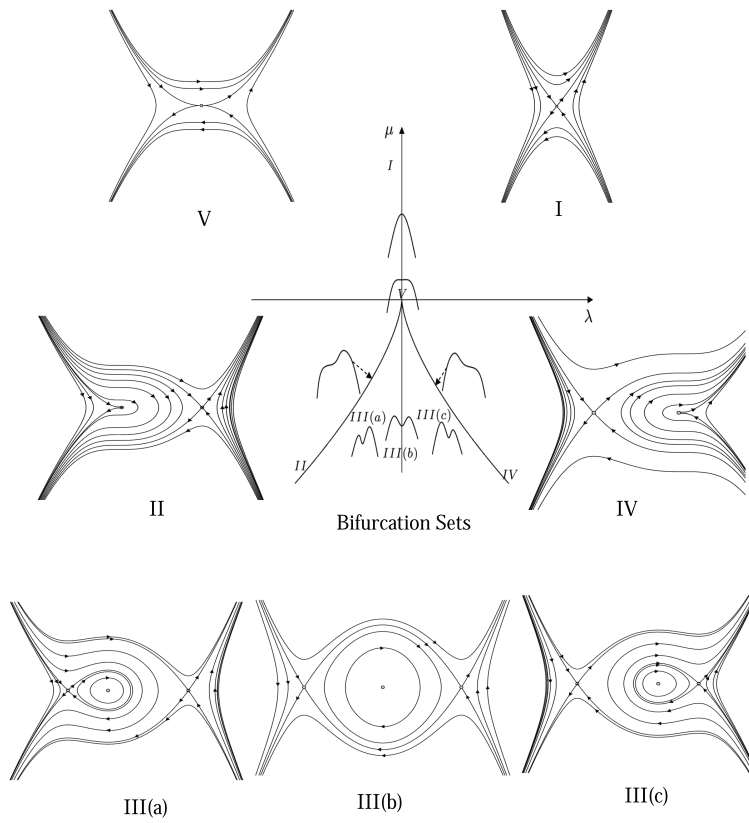


Figure 1: Bifurcation set and the typical phase portraits of equation (9) with $\alpha + \beta^2 > 0$ corresponding to different parametric regions I-V.

with oval of periodic orbit. The rest of trajectories are unbounded (see Figure 1 (III(a), III(b))).

- (4) If $\lambda^2 < -4\mu^3/27$, $\lambda = 0$, ($g_1^2 < (c^2 + 4g_2)^3/27$, $g_1 = 0$) (region III(c)), then the potential function (10) again has a minimum and two maximum points which correspond to a center and two saddle points of (9) respectively, but the values of potential function at maximum points are equal. The corresponding system (9) has a pair of heteroclinic orbits which is filled with oval of periodic orbits. The rest of trajectories are unbounded (see Figure 1 (III(c))).
- (5) If $\lambda = \mu = 0$, ($g_1 = c^2 + 4g_2 = 0$) (region V), then the potential function (10) has a degenerate maximum point, and the corresponding system (9) has a saddle point and all the trajectories are unbounded (see Figure 1 (V)).

Case II: ($\alpha + \beta^2 < 0$).

In this case trajectories of the system (9) are bounded, since the potential function F in the equation (10) is a polynomial of order four and the coefficient of x_1^4 is positive. It is easy to see that the only non-degenerate critical point of F in region *I* (outside of the cusp) is a minimum point and the corresponding system (9) has a global center (a band of periodic orbits filling the whole phase plane). Along the cusp (region *II*) the potential function (10) has a minimum and an inflection point which correspond to center and a cusp of system (9). The global phase portrait of (9) consists of a cuspidal loop and two band of periodic orbits, one inside and the other outside of the cuspidal loop. Inside the cusp (region *III*) the potential function (10) always has two non-degenerate minimum points and a non-degenerate maximum point between them which correspond to two centers and a saddle point for (9). The global phase portrait of the system (9) consists of two pairs of orbits homoclinic to the saddle point, two bands of periodic orbits inside each homoclinic orbits and a band of periodic orbits outside the double homoclinic orbit. In region *V* ($\lambda = \mu = 0$) the potential function (10) has a degenerate minimum point which correspond to global center of the system (10). Bifurcation set and graph of typical potential function and the corresponding phase portrait of the system (9) for different parametric regions are given in Figure 2.

Therefore we have proved:

Theorem 2.2. Consider the system (9) and assume that $\alpha + \beta^2 < 0$. In this case all trajectories of (10) are bounded. Further we have:

- (1) If $\lambda^2 > -4\mu^3/27$, ($g_1^2 > (c^2 + 4g_2)^3/27$) (region I), the potential function (10) has only one minimum point and the corresponding system (9) has a global center and all trajectories are periodic (see Figure 2 (I)).
- (2) If $\lambda^2 = -4\mu^3/27$, $\lambda \neq 0$ ($g_1^2 = (c^2 + 4g_2)^3/27$, $g_1 \neq 0$) (region II and IV), the potential function (10) has an inflection point and a minimum point and

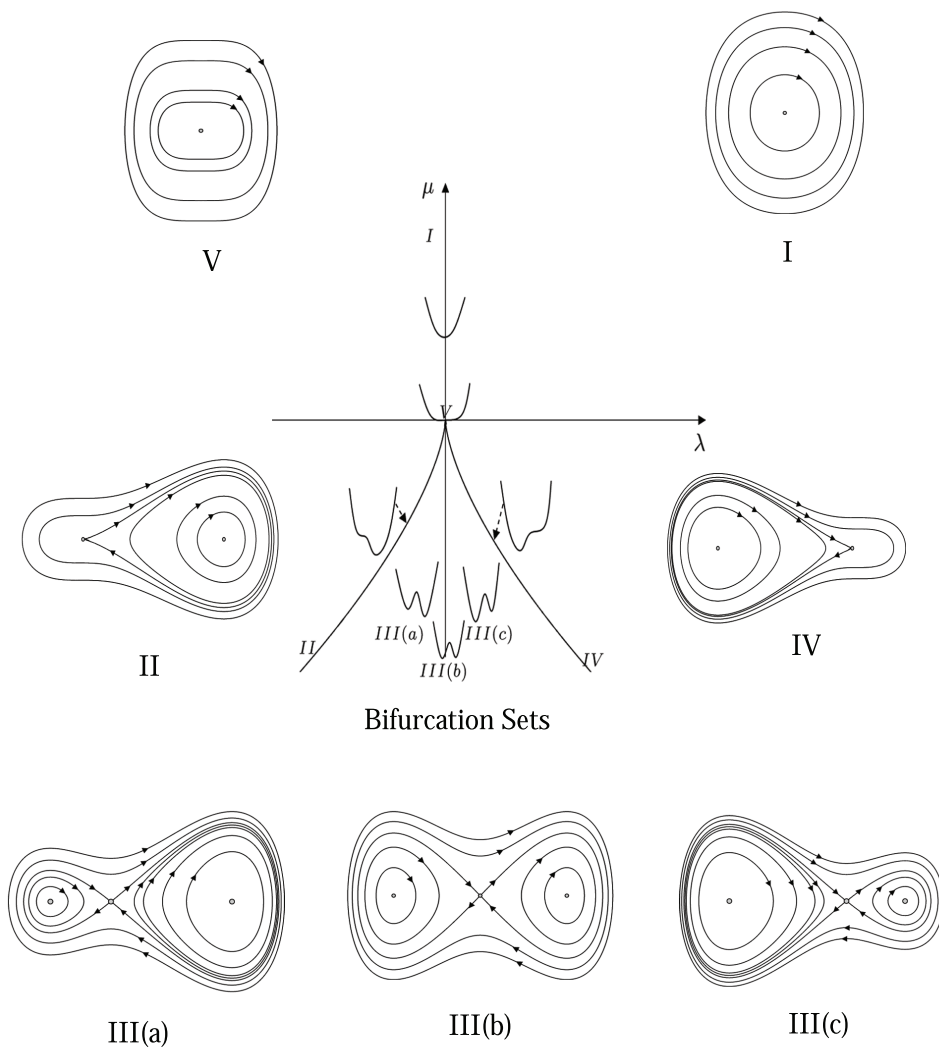


Figure 2: Bifurcation set and the typical phase portraits of equation (9) with $\alpha + \beta^2 < 0$ corresponding to different parametric regions $I-V$.

the corresponding system (9) has a center and a cusp point. Global phase portrait of (10) consists of a center, cuspidal loop and two bands of periodic orbits one inside the cuspidal loop and the others outside of the cuspidal loop (see Figure 2 (II, IV)).

- (3) If $\lambda^2 < -4\mu^3/27$, $\lambda \neq 0$ ($g_1^2 < (c^2 + 4g_2)^3/27$, $g_1 \neq 0$) (region III(a,b,c)), the potential function has a maximum and two minimum points, which correspond to a saddle point and two centers of the system (10). Global phase portrait of (9) consists of a double homoclinic orbit to the saddle point and two bands of periodic orbits each encircling the centers inside the double homoclinic loop and a band of periodic orbits outside the double homoclinic loop (see Figure 2 (III(a, b, c))).
- (4) If $\lambda = \mu = 0$, ($g_1 = c^2 + 4g_2 = 0$) (region V), the potential function has a degenerate minimum point, and the corresponding system (10) has a global center and all trajectories are periodic (see Figure 2 (V)).

3. The Numerical Simulation of Bounded Travelling Waves

It is well known that the bounded travelling waves $v(\xi)$ of the system (1) correspond to the bounded integral curves of the equation (6) which in turn correspond to the bounded orbits of the system (9). In Lemma 1 and Lemma 2, we have classified all bounded integral curves of the system (9). In this section we give numerical simulation for a typical member of bounded travelling waves of the system (1) in form of $v(x, t) = v(x - ct) = v(\xi)$ as follows:

Case I: Homoclinic orbits. These orbits only exist in regions $III(a, c)$ when $\alpha + \beta^2 > 0$ and in regions $III(a, b, c)$ when $\alpha + \beta^2 < 0$. Homoclinic orbits of the system (9) correspond to solitary travelling waves of (1). Let $g_1 = 1.2$, $g_2 = 0$, $c = 2$, $\alpha = \beta = 1$ which correspond to a point in region $III(c)$ in Figure 1. Now we consider the system (8) and choose initial conditions $v(0) = -0.9130466760$, $v'(0) = 0$ so that they lie on the homoclinic orbit. In physics this type of travelling waves are called solitary wave with valley form (see Figure 3(a)). Now let $g_1 = -1.2$, $g_2 = 0$, $c = 2$, $\alpha = \beta = 1$ which correspond to a point in parametric region $III(c)$ in Figure 1. Again we use initial conditions to be on the homoclinic orbit of the system (8). Let $v(0) = -1.086953458$, $v'(0) = 0$. This type of travelling wave in physics are called solitary wave with peak form (see Figure 3(b)).

Case II: Cuspidal loops. These orbits only exist in regions (II) and (IV) when $\alpha + \beta^2 > 0$. Cuspidal loop of the system (8) again correspond to solitary travelling wave of the system (1). As in previous part we choose two set of parameters $g_1 = \pm 1.5396$, $g_2 = 0$, $c = 2$, $\beta = 0$ and $\alpha = -2$ on different branches of the cusp in parametric regions II and IV in Figure 2. Positive g_1 (region IV)

correspond to solitary wave with valley form and negative g_1 (region II) correspond to solitary wave with peak form. Now we consider the system (8) and choose initial conditions to be on their cuspidal loops. For the first case ($g_1 > 0$) let $v(0) = 2.732050$, $v'(0) = 0$ and for the second case ($g_1 < 0$) let $v(0) = -0.732050$, $v'(0) = 0$ (see Figure 4(a,b)). We notice the difference between solitary waves in Figures 3 and 4 which show their asymptotic behavior as $t \rightarrow \pm\infty$. In Figure 3 stable and unstable manifolds of equilibrium point intersect transversally but in Figure 4 they intersect tangentially.

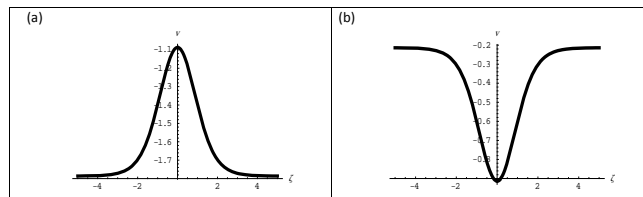


Figure 3: Simulation of solitary waves corresponding to the homoclinic orbits of the equation (8). (a) Solitary wave of peak form, (b) Solitary wave of valley type.

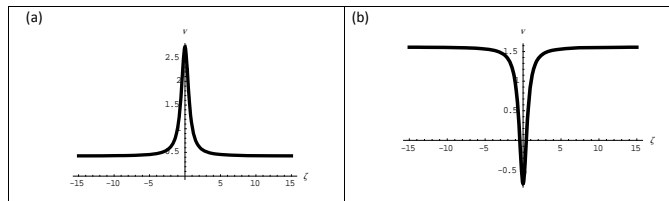


Figure 4: Simulation of the cusped solitary waves corresponding to cuspidal loops of the equation(8). (a) Solitary wave of peak form, (b) Solitary wave of valley type.

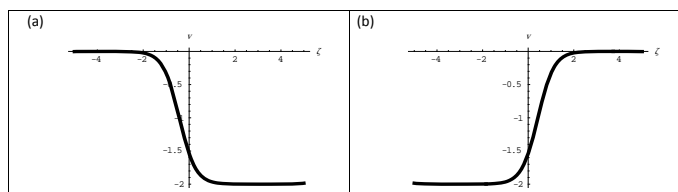


Figure 5: Simulation of the kink and anti-kink waves corresponding to the heteroclinic orbits of the equation(8). (a) Anti-kink waves, (b) kink waves

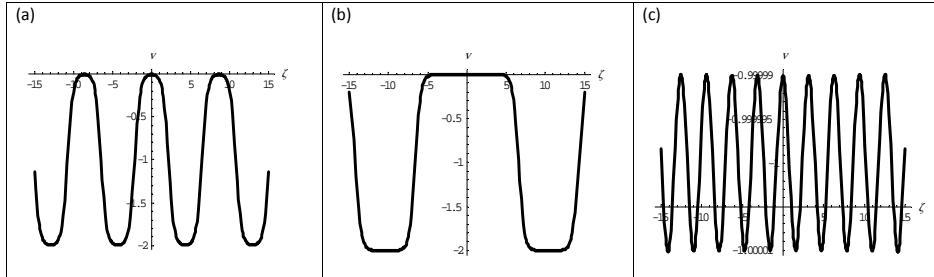


Figure 6: Simulation of periodic waves corresponding to periodic orbits inside heteroclinic cycle of the equation(8). (a) medium period, (b) long period , (c) Short period.

Case III: Heteroclinic orbits. These orbits exist only in region $(III(b))$ when $\alpha + \beta^2 > 0$. Upper and lower heteroclinic orbits of the system (8) correspond to kink and anti-kink travelling waves of system (1) respectively. Again we consider the system (8) and choose $g_1 = g_2 = 0, c = 2, \alpha = \beta = 1$ which correspond to a point in parametric region $III(b)$ in Figure 1. As we have mentioned above in this case we have heteroclinic orbits connected to saddle points $(0, 0)$ and $(-2, 0)$. Now we use the initial conditions $v(0) = -1.541196100, v'(0) = 1$ and $v(0) = -1.541196100, v'(0) = -1$ on upper and lower heteroclinic orbits respectively and we get Figure 4(a,b).

Case IV: Periodic orbits. These periodic orbits are global centers (regions I and V when $\alpha + \beta^2 < 0$) or local centers which lie inside homoclinic orbits (regions $III(a, b, c)$ when $\alpha + \beta^2 < 0$ and regions $III(a, c)$ when $\alpha + \beta^2 > 0$), inside and outside of cuspidal loops (regions II and IV when $\alpha + \beta^2 < 0$) and inside heteroclinic cycles (region $III(b)$ when $\alpha + \beta^2 > 0$). Periodic orbits of the system (1) correspond to periodic travelling waves of the system (1). Here we choose a periodic orbit inside the heteroclinic orbits in region $III(b)$ in Figure 1. Of course we could choose a global center or a periodic orbit inside homoclinic orbits, periodic orbit inside and outside of cupidal loops as well, but the figures are qualitatively the same. Let $g_1 = g_2 = 0, c = 2, \alpha = \beta = 1$. Heteroclinic orbit corresponding to these set of parameters passes through saddle points $(0, 0)$ and $(-2, 0)$ and include the center $(-1, 0)$ of the system(8). We choose three sets of initial conditions $v(0) = -0.99999, v'(0) = 0, v(0) = -3 \times 10^{-11}, v'(0) = 0$ and $v(0) = -0.0009, v'(0) = 0$, close to center $(-1, 0)$, somewhere in middle of heteroclinic cycle and very close to heteroclinic orbit respectively (see Figure 5(a,b,c)). We notice that period of these periodic orbits increases as we move away from the center toward the heteroclinic orbits.

4. Explicit Formulas for Bounded Integral Curves of (9)

In this section we give explicit formulas for some bounded closed integral curves of the system (9). Let us assume that $(a, 0)$, $(b, 0)$ and $(c, 0)$ are equilibrium points of the system (9), so that $a < b < c$. We describe each of these curves according to classification given in previous section.

Case I: Homoclinic orbits:

First we consider Homoclinic orbit in region $III(a)$ of Figure 1 ($\alpha + \beta^2 > 0$). In this case $(a, 0)$, $(c, 0)$ are saddle points while $(b, 0)$ is a center and the integral curve is homoclinic to $(a, 0)$. Therefore it is given by $H(x_1, x_2) = H(a, 0)$. Now we set

$$\begin{aligned} G(x_1, x_2) &= H(x_1, x_2) - H(a, 0) \\ &= x_2^2/2 - 2[x_1^4 - a^4 + 2\mu(x_1^2 - a^2) + 4\lambda(x_1 - a)]/(\alpha + \beta^2). \end{aligned}$$

But $(a, 0)$ is a multiple root of $G(x_1, 0)$, since by definition it is clear that $G(a, 0) = 0$ and moreover $(a, 0)$ is a critical point of (9). Therefore

$$G(x_1, 0) = -2(x_1 - a)^2(x_1 - a^-)(x_1 - a^+)/(\alpha + \beta^2), \quad (12)$$

where a^+ and a^- are roots of quadratic polynomial $x_1^2 + 2ax_1 + 2\mu + 3a^2$ and are given by

$$a^\pm = -a \pm \sqrt{-2(\mu + a^2)} = -a \pm \sqrt{2\lambda}a.$$

Therefore along this homoclinic orbit we have

$$x_2 = 2\sqrt{(x_1 - a)^2(a^+ - x_1)(a^- - x_1)/(\alpha + \beta^2)},$$

where $a^+ > a^- > x_1 > a$. Now by using the equation (9) we have

$$\frac{\sqrt{\alpha + \beta^2}}{2} \int_{\zeta}^0 d\sigma = \int_{x_1}^{a^-} \frac{dv}{\sqrt{(v - a)^2(a^+ - v)(a^- - v)}}, \quad (13)$$

after integrating above integral we find that

$$x_1(\zeta) = a + \frac{2(a^+ - a)(a^- - a)}{a^- + a^+ - 2a + (a^+ - a^-) \cosh(\theta_1 \zeta)},$$

where $\theta_1 = \sqrt{(\alpha + \beta^2)(a^- - a)(a^+ - a)}/2$. Therefore, the equation (1) has solitary wave solution with peak form. If the integral curve is homoclinic to $(c, 0)$, corresponding to region $III(c)$ in Figure 1 just we need to interchange role of c and a in above. Therefore, the equation (1) has a solitary wave solution with valley form.

Now we consider Homoclinic orbits in region III of Figure 2 ($\alpha + \beta^2 < 0$). In this case the critical points of (9) are as follows: $(b, 0)$ is a saddle point while $(a, 0)$

and $(c, 0)$ are centers and the integral curves are homoclinic to $(b, 0)$. Similar to above, along these homoclinic orbits we have

$$x_2 = 2\sqrt{-(x_1 - b)^2(a^+ - x_1)(x_1 - a^-)/(\alpha + \beta^2)},$$

where $b^\pm = -b \pm \sqrt{-2(\mu + b^2)}$ and $b^- < x_1 < b^+$. Therefore by using the equation (9) along the right branch of the double homoclinic orbit we get

$$\frac{\sqrt{-(\alpha + \beta^2)}}{2} \int_{\xi}^0 d\sigma = \int_{x_1}^{b^+} \frac{dv}{\sqrt{(v - b)^2(b^+ - v)(v - b^-)}}.$$

After integration and some simplification we get

$$x_1(\xi) = b + \frac{2(b^+ - b)(b^- - b)}{2b - b^+ - b^- + (b^+ - b^-) \cosh(\theta_2 \xi)},$$

where $\theta_2 = \sqrt{(\alpha + \beta^2)(b - b^-)(b^+ - b)}/2$. Therefore, the equation (1) has a solitary wave solution with peak and valley form.

Similarly for the left branch of the homoclinic orbit in region *III* of Figure 2 we get

$$x_1(\xi) = b + \frac{2(b^+ - b)(b^- - b)}{b^+ - b^- - 2b + (b^+ - b^-) \cosh(\theta_2 \xi)},$$

which correspond to the solitary wave solution with peak and valley form of the equation (1).

Case II: Cuspidal loop

Cuspidal loops exist only when $\alpha + \beta^2 < 0$. We consider Cuspidal loop in regions *II* or *IV* of Figure 2. In this case equilibrium points are $(a, 0)$ and $(b, 0)$ so that $(a, 0)$ is a cusp and $(b, 0)$ is a center. Therefore there are two cases:

1. $a > 0$ and $a > b$, where $b = -2a = -\sqrt{-\mu/3}$ which correspond to region *IV* in Figure 2.
2. $a < 0$ and $a < b$, where $b = -2a = \sqrt{-\mu/3}$ which correspond to region *II* in Figure 2.

Homoclinic cuspidal loop through $(a, 0)$ also passes through the point $(-3a, 0)$ on x -axis. Therefore

$$G(x_1, x_2) = H(x_1, x_2) - H(a, 0) = x_2^2/2 - 2(x_1 - a)^3(x_1 + 3a)/(\alpha + \beta^2),$$

thus $G(x_1, 0) = -2(x_1 - a)^3(x_1 + 3a)/(\alpha + \beta^2)$. Along the cuspidal loop we have

$$x_2 = \pm 2\sqrt{(a - x_1)^3(x_1 + 3a)/(\alpha + \beta^2)}.$$

Now by using the equation (9) we have

$$\frac{\sqrt{-(\alpha + \beta^2)}}{2} \int_0^\zeta d\sigma = \int_{-3a}^{x_1} \frac{dx}{(a-x)\sqrt{2(a-x)(x+3a)}},$$

where for cuspidal loop in region *II*, we have $a < 0$ and $a < x_1 < -3a$ and for cuspidal loop in region *IV* we have $a > 0$ and $-3a < x_1 < a$. Therefore we get

$$x_1(\zeta) = \frac{a(3 + 2a^2(\alpha + \beta^2)\zeta^2)}{2a^2(\alpha + \beta^2)\zeta^2 - 1}.$$

Case III: Heteroclinic orbit

Heteroclinic orbit exists only in region *III(b)* of Figure 1 for $\alpha + \beta^2 > 0$. Similar to homoclinic case, $(a, 0)$ and $(c, 0)$ are saddle points while $(b, 0)$ is a center, but in this case there is an additional symmetry so that $-a = c = \sqrt{-\mu}$. Therefore the equation (12) becomes

$$G(x_1, 0) = -2(x_1^2 - a^2)^2 / (\alpha + \beta^2),$$

where $a < x_1 < c$ and the equation(13) becomes

$$\frac{2}{\sqrt{\alpha + \beta^2}} \int_0^\zeta d\sigma = \pm \int_0^{x_1} \frac{dx}{x^2 + \mu}.$$

Therefore

$$x_1(\zeta) = \pm a \tanh\left(2a\zeta / \sqrt{\alpha + \beta^2}\right),$$

in which positive sign corresponds to upper branch and negative sign corresponds to lower branch of heteroclinic cycle which in turn correspond to anti-kink and kink travelling wave of the system (1).

Case IV: Periodic orbits

Periodic orbits exist when either $\alpha + \beta^2$ is positive or is negative. Here we only consider periodic orbits of (9) which are located in different regions of Figure 2 ($\alpha + \beta^2 < 0$). Suppose that the periodic orbits passes through $(a, 0)$ and $(b, 0)$ so that $a < b$. Therefore this periodic orbit lies on level curve $H(x_1, x_2) = H(b, 0) = h$ where H is given by (10). As before define $G(x_1, 0) = H(x_1, 0) - H(b, 0)$. Then, $G(x_1, 0)$ is a polynomial of order four with respect to x_1 , where a and b are their roots. There will be two distinct cases; $G(x_1, 0)$ has either two or four real roots (counting the multiplicity).

Two real roots: We consider a periodic orbit in either of regions *I*, *II*, *IV* or *V* of Figure 2. In these cases

$$G(x_1, 0) = -2(a - x_1)(x_1 - b)((x - \delta)^2 + \gamma^2) / (\alpha + \beta^2).$$

Therefore along the periodic orbit we have

$$x_2 = \pm \sqrt{-2(a - x_1)(x_1 - b)((x - \delta)^2 + \gamma^2) / (\alpha + \beta^2)},$$

where

$$\delta = -(a + b)/2, \quad \gamma^2 = -2\mu + 3\delta^2 - ab, \quad 2\lambda/\delta = 2\mu + a^2 + b^2.$$

Now by using (9) and integral tables for elliptic integrals (see [1]) we have

$$\frac{\sqrt{-(\alpha + \beta^2)}}{2} \int_0^\zeta d\sigma = \int_b^{x_1} \frac{dx}{\sqrt{(a-x)(x-b)((x-\delta)^2 + \gamma^2)}} = gcn^{-1}(\cos \phi, k),$$

where cn^{-1} is the inverse Jacobian elliptic function with the modulus k (see [1]) and

$$A^2 = (a - \delta)^2 + \gamma^2, \quad B^2 = (b - \delta)^2 + \gamma^2, \quad g = 1/\sqrt{AB},$$

$$k^2 = \frac{(a - b)^2 - (A - B)^2}{4AB}, \quad \phi = \cos^{-1} \left(\frac{(a - x_1)B - (x_1 - b)A}{(a - x_1)B + (x_1 - b)A} \right).$$

Therefore we have

$$x_1(\zeta) = \frac{(aA + \delta B) - (aB - \delta A)cn(\Omega\zeta, k)}{(A + B) + (A_B)cn(\Omega\zeta, k)},$$

where cn is the Jacobian elliptic function with modulus k (see [1]) and $\Omega = \sqrt{-(\alpha + \beta^2)}/(2g)$.

Four real roots: Let a, b, c and d be real roots of $G(x_1, 0) = 0, a < b < c < d$ and the periodic orbit is passing through $(a, 0)$ and $(b, 0)$. Therefore along the periodic orbits, $a \leq x_1 < b < c < d$ and we have

$$x_2 = \pm 2\sqrt{-(c - x_1)(d - x_1)(x_1 - a)(b - x_1)/(\alpha + \beta^2)}.$$

Now by using (9) and integral tables (see [1]) we obtain

$$\frac{\sqrt{-(\alpha + \beta^2)}}{2} \int_\xi^0 d\sigma = \int_{x_1}^b \frac{dv}{\sqrt{(d-v)(c-v)(v-a)(b-v)}} = gsn^{-1}(\sin \phi, k),$$

where sn^{-1} is the inverse Jacobian elliptic function with the modulus k (see [1]) and

$$\phi = \sin^{-1} \left(\sqrt{\frac{(c - a)(b - x_1)}{(b - a)(c - x_1)}} \right), \quad k^2 = \frac{(d - c)(b - a)}{(d - b)(c - a)}, \quad g = \frac{2}{\sqrt{(d - b)(c - a)}}.$$

Therefore this periodic orbit is given by

$$x_1(\zeta) = a + \frac{(d - c)(b - a)sn^2(\Omega\zeta, k)}{(d - b) + (b - a)sn^2(\Omega\zeta, k)},$$

where sn is the Jacobian elliptic function with modulus k (see [1]) and $\Omega = \sqrt{-(\alpha + \beta^2)}/(2g)$. Now if we consider the periodic orbits inside the right branch

of double homoclinic orbits for which periodic orbits are passing through $(c, 0)$ and $(d, 0)$ with $a < b < c < x_1 \leq d$ then by using a similar procedure we get

$$x_1(\zeta) = c + \frac{(d-c)(c-b)sn^2(\Omega\zeta, k)}{(d-b) + (d-c)sn^2(\Omega\zeta, k)}.$$

There are other cases which correspond to periodic orbits inside homoclinic and heteroclinic orbits in Figure 1 with $\alpha + \beta^2 > 0$ which can be treated similarly and omitted for the sake of brevity.

Acknowledgement. The first author was supported in part by the University of Kashan under Grant No. 572769/1.

Conflicts of Interest. The authors declare that there are no conflicts of interest regarding the publication of this article.

References

- [1] P. F. Byrd and M. D. Fridman, *Handbook of Elliptic Integrals for Engineers and Scientists*, Springer-Verlag, New York-Heidelberg, 1971.
- [2] En. G. Fan, *Integrable Systems and Computer Algebra*, Science Press, 2004.
- [3] E. Fan, Soliton solutions for a generalized Hirota-Satsuma coupled KdV equation and a coupled MKdV equation, *Phys. Lett. A* **282** (2001) 18–22.
- [4] D. Feng, J. Lu, J. Li and T. He, Bifurcation studies on travelling wave solutions for nonlinear intensity Klein-Gordon equation, *Appl. Math. Comput.* **189** (2007) 271–284.
- [5] J. K. Hale and H. Kocak, *Dynamics and Bifurcation*, Springer-Verlag, New York, 1991.
- [6] J. H. He, Application of homotopy perturbation method to nonlinear wave equations, *Chaos, Solitons & Fractals* **26** (2005) 695–700.
- [7] R. Hirota, Exact solution of the Korteweg-de Vries equation for multiple collisions of solitons, *Phys. Rev. Lett.* **27** (1971) 1192–1194.
- [8] J. Q. Hu, An algebraic method exactly solving two high-dimensional nonlinear evolution equations, *Chaos, Solitons & Fractals* **23** (2005) 391–398.
- [9] B. Jiang, Y. Lu, J. Zhang and Q. Bi, Bifurcations and some new traveling wave solutions for the CH- γ equation, *Appl. Math. Comput.* **228** (2014) 220–233.
- [10] M. Khalfallah, Exact traveling wave solutions of the Boussinesq-Burger equation, *Math. Comput. Modelling* **49** (2009) 666–671.

-
- [11] J. B. Li and Y. S. Li, Bifurcations of travelling wave solutions for a two-component Camassa–Holm equation, *Acta Math. Sin. (Engl. Ser.)* **24** (2008) 1319–1330.
- [12] Sh. Liu, Z. Fu, Sh. Liu and Q. Zhao, Jacobi elliptic function expansion method and periodic wave solutions of nonlinear wave equations, *Phys. Lett. A* **285** (2001) 69–74.
- [13] S. Y. Lou and X. Y. Tang, *Nonlinear Mathematical and Physical Methods*, Science Press, 2006.
- [14] R. M. Miura, *Backlund Transformation, the Inverse Scattering Method, Solitons, and their Applications*, Springer-Verlage, Berlin, 1976.
- [15] A. S. A. Rady and M. Khalfallah, On soliton solutions for Boussinesq-Burgers equations, *Commun. Nonlinear Sci. Numer. Simul.* **15** (2010) 886–894.
- [16] M. Wang, Exact solutions for a compound KdV-Burgers equation, *Phys. Lett. A* **213** (1996) 279–287.
- [17] J. Weiss, M. Tabor and G. Carnevale, The painleve property for partial differential equations, *J. Math. Phys.* **24** (1983) 522–526.
- [18] Ch. Yan, A simple transformation for nonlinear waves, *Phys. Lett. A* **224** (1996) 77–84.
- [19] H. R. Z. Zangeneh, R. Kazemi and M. Mosaddeghi, Classification of bounded travelling wave solutions of the generalized Zakharov equation, *Iran. J. Sci. Technol. Trans. A Sci.* **38** (2014) 355–364.
- [20] K. Zhang and J. Han, Bifurcations of traveling wave solutions for the $(2 + 1)$ -dimensional generalized asymmetric Nizhnik-Novikov-Veselov equation, *Appl. Math. Comput.* **251** (2015) 108–117.

Rasool Kazemi
Department of Pure Mathematics,
University of Kashan,
Kashan, I. R. Iran
E-mail: r.kazemi@kashanu.ac.ir

Masoud Mosaddeghi
Department of Mathematical Sciences,
Isfahan University of Technology,
Isfahan, I. R. Iran
E-mail: m.mosaddeghi@math.iut.ac.ir